

# Optimum settings for PID control of nonlinear systems

R. Vrabel

*Slovak University of Technology in Bratislava, Institute of Applied Informatics,  
Automation and Mechatronics, Bottova 25, 917 01 Trnava, Slovakia*

---

## Abstract

This paper investigates the application of piecewise linear approximation for the control of nonlinear systems, particularly focusing on the effective linearization of systems modeled by the differential equation  $y^{(n)} + f(y, y', \dots, y^{(n-1)}) = u(t)$ . We explore the use of PID controllers in conjunction with piecewise linearization, tackling the challenges of nonlinear dynamics by dividing the function  $f$  into smaller regions or simplices over a predefined compact set  $D \subset \mathbb{R}^n$ . The parameter  $h$  determines the number of linear pieces and influences the approximation accuracy. By increasing  $h$ , the system's behavior increasingly mirrors that of the original nonlinear system, leading to enhanced performance of the control system. The paper further discusses the optimization of PID controller parameters through the Particle Swarm Optimization method, with a focus on minimizing the ITAE and ISO criteria. Numerical simulations demonstrate the efficacy of the approach, highlighting the trade-off between computational complexity and approximation accuracy in the context of control system design.

*Keywords:* Nonlinear system; PID control; Particle Swarm Optimization method.

---

## 1. Introduction

Transfer functions are a fundamental tool in linear system analysis, providing a frequency-domain representation that simplifies the study of system behavior. However, for nonlinear systems, the concept of a transfer function is not directly applicable due to the system's inherent nonlinearities. De-

---

*Email address:* robert.vrabel@stuba.sk (R. Vrabel)

spite this, several methodologies have been developed to extend the transfer function concept to nonlinear systems [15].

The describing function method approximates certain nonlinear systems by linearizing them around a specific operating point, particularly for systems with sinusoidal inputs. This approach provides an approximate frequency-domain analysis but is limited to specific types of nonlinearities and input signals.

The Volterra series generalizes the concept of transfer functions to nonlinear systems by representing the system's output as a series of multidimensional convolutions of the input. Each term in the series corresponds to a higher-order frequency response function, capturing the system's nonlinear behavior. This method is particularly useful for weakly nonlinear systems.

Relatively recent research has introduced the concept of quasi-linear transfer functions, which aim to characterize the output frequency behavior of nonlinear systems. This method provides a new perspective on analyzing nonlinear systems in the frequency domain.

Another approach involves extending system-level synthesis methods to polynomial dynamical systems, yielding finite impulse response, time-invariant, closed-loop transfer functions with guaranteed disturbance cancellation. This generalizes feedback linearization to enable partial feedback linearization over a finite-time horizon.

These resources offer a comprehensive overview of the methodologies developed to analyze nonlinear systems using concepts analogous to transfer functions.

The proportional-integral-derivative (PID) controller is a cornerstone in feedback control systems due to its simplicity, effectiveness, and versatility. It is a general-purpose algorithm used to regulate processes in a wide variety of applications, from industrial automation to robotics, avionics, and beyond. The controller works by continuously adjusting the control input to minimize the error between a desired setpoint and the actual process output. The optimization of PID control parameters for nonlinear systems is more challenging than for linear systems because nonlinearities can cause unpredictable behavior, such as oscillations (limit cycles, chaos-induced oscillations, self-sustained oscillations), instability, or slow convergence. Nonlinear systems often exhibit behavior such as saturation, dead-zone, hysteresis, and time-varying dynamics that complicate the control process. Traditional PID controllers are designed for linear systems, and their performance in nonlinear systems may degrade due to the inability to model nonlinearities directly.

Thus, optimal PID tuning in nonlinear systems is crucial for avoiding issues like overshoot, oscillations, or slow response. To achieve optimal PID performance in nonlinear systems, several methods and strategies are employed.

In some cases, the nonlinear system can be linearized around an operating point. This simplified linear model can then be used to apply classical PID tuning methods. However, this method only works for relatively small deviations from the operating point and does not always capture the full nonlinear behavior (if the equilibrium point is not hyperbolic, for example).

Adaptive PID controllers adjust the PID parameters in real-time based on the changing dynamics of the nonlinear system. This approach is useful when the nonlinear system's behavior changes with time or operating conditions. Adaptive methods can be based on model reference adaptive control (MRAC), where the controller parameters are modified to match a desired reference model in real-time to account for changing system dynamics or operating conditions.

Gain scheduling involves adjusting the PID parameters based on the operating conditions of the nonlinear system. This approach requires identifying different operating regimes of the system, each of which may need different PID gains. For example, the PID gains can be varied depending on system speed, temperature, or load.

Optimization algorithms such as Genetic Algorithms, Particle Swarm Optimization (PSO), and Simulated Annealing can be used to find the optimal PID parameters for nonlinear systems by minimizing a cost function, typically involving criteria like settling time, overshoot, steady-state error and control effort.

In some cases, using a pure PID controller may not be effective for nonlinear systems. In such cases, nonlinear control methods such as fuzzy logic controllers, sliding mode controllers, or backstepping control are often considered. However, PID controllers can still be used in combination with these methods to improve performance.

By incorporating fuzzy logic into the PID structure, the controller can handle nonlinearities more effectively. The fuzzy logic component allows the controller to adjust its behavior based on the input-output relationship, compensating for nonlinearities.

Neural networks can also be used to tune the PID parameters or modify the control strategy. This technique can handle complex nonlinearities by learning from data.

Book [2] discusses PID control design and optimization for various sys-

tems, including nonlinear systems, with practical insights into tuning and implementation. A widely-used textbook [11] offers a solid foundation for both linear and nonlinear control systems, including techniques for PID control of nonlinear systems. Book [12] provides a detailed treatment of control system analysis and design, including PID control and nonlinear system behavior.

The Particle Swarm Optimization (PSO) algorithm as initially developed by James Kennedy and Russell Eberhart [7, 9, 16], inspired by the collective movement of bird flocks and fish schools. The idea was to simulate the social behavior of these animals to solve optimization problems. The initial paper [7] presented the basic PSO model, which was intended to simulate the social behavior of organisms in nature and solve nonlinear optimization problems. PSO's history is characterized by its rapid evolution and widespread adoption in diverse fields. Initially designed for simple optimization problems, it has since become a robust tool for solving complex, multi-dimensional, and dynamic optimization challenges. Researchers continue to explore new variants and applications, ensuring PSO's relevance in modern computational intelligence. Researchers began developing PSO variants for multi-objective optimization problems [5, 6]. Multi-objective PSO methods have been widely adopted in real-world engineering and scientific optimization tasks. Several studies started combining PSO with other optimization algorithms (such as genetic algorithms or simulated annealing) to create hybrid models that could perform better on certain problems. PSO was adapted for constrained optimization problems, where researchers developed specific mechanisms to handle constraints in the search space [14]. PSO has gained widespread use in machine learning for tasks such as feature selection, training deep learning networks, and hyperparameter tuning. PSO has been applied in various industries such as robotics, control systems, image processing, and power systems optimization. In response to large-scale optimization problems, parallel and distributed PSO algorithms have been developed to take advantage of modern computing architectures [17]. The basic PSO algorithm has been modified in several ways to limit the particle movement and avoid divergence, to control the influence of previous velocity on the next velocity, improving convergence and exploration/exploitation balance and adjusting these parameters to balance local search (individual experience) and global search (group experience).

The objective of this paper is to develop a methodology for the analysis and synthesis of control circuits by approximating a nonlinear system in a

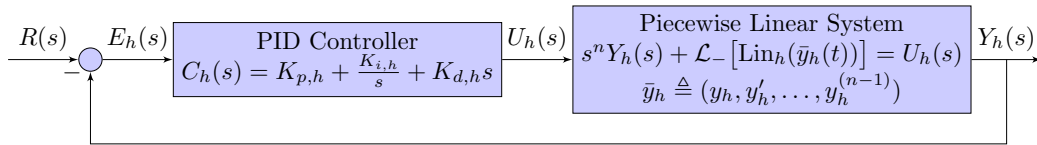


Figure 1: Feedback control system with piecewise linear approximation of the nonlinear system.

feedback configuration, as illustrated in the accompanying schematic (Figure 1), using transfer functions derived via piecewise linear, more precisely affine approximation. We demonstrate that, under specific assumptions, the solutions of the sequence of linearized systems are well-defined over the entire real-time axis and uniformly converge to the solution of the original nonlinear model. Similarly, the corresponding transfer functions exhibit analogous convergence behavior, and the limit function can be legitimately interpreted as the transfer function of the nonlinear system, the formula 7.

In the subsequent stage of the study, we address the design of PID controller parameters ( $K_p, K_i, K_d$ ) through a cost function minimization approach utilizing PSO algorithm, implemented via the `pyswarm` module which offers a flexible and efficient way to use PSO in Python. The efficacy of the proposed methodology is validated by comparing its performance against traditional controller parameter tuning methods, such as closed-loop tuning, in the context of a linear time-varying system. Furthermore, in Subsection 8.2, we illustrate the application of the proposed approach to a nonlinear system. First, let us introduce two important technical results that will be used in the proofs of existence and uniqueness of the solutions, as well as their uniform convergence.

## 2. Banach Contraction Principle and Gronwall Inequality

Both the Banach Contraction Principle [3] and Gronwall Inequality [8] are fundamental tools in analysis, particularly in the study of differential equations, stability analysis, and control theory. They are often applied to prove existence and uniqueness of solutions, estimate bounds on solutions, and establish stability results.

**Theorem 1 (Banach Contraction Principle).** *Let  $(X, d)$  be a complete metric space, and let  $T : X \mapsto X$  be a contraction mapping, meaning there*

exists a constant  $c \in [0, 1)$  such that

$$d(T(x), T(y)) \leq c \cdot d(x, y), \quad \text{for all } x, y \in X.$$

Then, there exists a unique point  $x^* \in X$  such that  $T(x^*) = x^*$ .

The Gronwall inequality is a key result used to derive bounds on solutions of differential inequalities. It provides a means to estimate the growth of a solution to a differential equation or an inequality, especially when the solution is constrained by an upper bound. There are several forms of Gronwall inequality, but one of the most common forms relevant to differential equations is the differential inequality form.

**Theorem 2.** *Suppose  $w(t)$  is a differentiable function on an interval  $[a, b]$ , and satisfies the following differential inequality*

$$\frac{dw(t)}{dt} \leq f(t)w(t) + g(t), \quad t \in [a, b],$$

where  $f(t)$  and  $g(t)$  are continuous functions.

Then,  $w(t)$  satisfies the following bound

$$w(t) \leq w(a) \exp\left(\int_a^t f(s) ds\right) + \int_a^t g(s) \exp\left(\int_s^t f(\tau) d\tau\right) ds.$$

### 3. Linear interpolation of $n$ -dimensional function $f$ over an $n$ -simplex

To prove the uniform convergence of piecewise linear approximations for a  $C^2$ -function  $f : \mathbb{R}^n \mapsto \mathbb{R}$ , we need to show that the sequence of piecewise linear functions converges uniformly to  $f$  as the partition of the domain becomes finer. In general, our considerations are valid for  $C^2$  functions (i.e. twice continuously differentiable function on  $\mathbb{R}^n$ ), but if it is possible to relax these assumptions in certain steps, we will do so.

Step 1: Define the Piecewise Linear Approximation

Let  $D \subseteq \mathbb{R}^n$  be a compact domain, and assume that  $f$  is differentiable on  $D$ . We define a sequence of piecewise linear approximations to  $f$ , denoted as  $\text{Lin}_h$ , constructed as follows:

1. Partition the domain: We partition the domain  $D$  into a grid of small regions, typically line segments (in  $\mathbb{R}^1$ ), triangles (in  $\mathbb{R}^2$ ), tetrahedrons (in  $\mathbb{R}^3$ ) or, in general,  $n$ -simplices (in  $\mathbb{R}^n$ ), such that the maximum diameter of the cells in the partition becomes arbitrarily small as  $h$  increases.

$\{h\}$  is an infinite and increasing sequence of natural numbers. Denote this partition as  $P_h$ , where the size of the cells  $C_{h,i}$ ,  $i = 1, 2, \dots, h$  in the partition decreases as  $h \rightarrow \infty$ . The  $n$ -simplex  $C_{h,i}$  is defined by its vertices  $\{P_{1h,i}, P_{2h,i}, \dots, P_{n+1h,i}\}$  and the function  $f$  is known at these vertices.

2. Linear approximation on each region: For each cell  $C_{h,i} \in P_h$ , we approximate  $f$  by a linear function  $\text{Lin}_{h,i}(y)$  that takes the values of  $f$  at the vertices of the cell. More precisely, on each cell  $C_{h,i}$ , we define  $\text{Lin}_{h,i}(y)$  by interpolating the values of  $f$  at the vertices of  $C_{h,i}$ .

The goal is to compute the value of the function  $\text{Lin}_{h,i}(y)$  at any point  $y$  within the simplex  $C_{h,i}$ .

In the case of an  $n$ -simplex, the coordinates  $\lambda_1, \lambda_2, \dots, \lambda_{n+1}$  of a point  $y$  inside the simplex can be expressed as the barycentric coordinates. These coordinates are non-negative and satisfy the condition

$$\sum_{i=1}^{n+1} \lambda_i = 1$$

The general form for the linear interpolation of the function  $f$  on  $C_{h,i}$  is

$$\text{Lin}_{h,i}(y) = \sum_{j=1}^{n+1} \lambda_j f(P_{jh,i}), \quad i = 1, 2, \dots, h$$

To compute the barycentric coordinates  $\lambda_1, \lambda_2, \dots, \lambda_{n+1}$  for a point  $y$ , we need to calculate the areas (or volumes, depending on the dimension) of the sub-simplices formed by  $y$  and the vertices of the simplex.

For a given point  $y$  inside the  $n$ -simplex  $C_{h,i}$ , the barycentric coordinates  $\lambda_j$  are proportional to the volume of the  $n - 1$ -simplex formed by excluding the vertex  $P_{jh,i}$ , and this is normalized by the volume of the full  $n$ -simplex.

The formula for the barycentric coordinate  $\lambda_j$  in terms of the volume is

$$\lambda_j = \frac{\text{Vol}(C_{h,i}^{(j)})}{\text{Vol}(C_{h,i})}$$

where

- $\text{Vol}(C_{h,i})$  is the volume of the  $n$ -simplex formed by the vertices  $P_{1h,i}, P_{2h,i}, \dots, P_{n+1h,i}$ .
- $\text{Vol}(C_{h,i}^{(j)})$  is the volume of the sub-simplex formed by the point  $y$  and all the vertices of the simplex except  $P_{jh,i}$ .

Thus,

$$\text{Lin}_h(y) \triangleq \{\text{Lin}_{h,i}(y) \mid i = 1, 2, \dots, h\} \quad (1)$$

represents piecewise linear approximation of the function  $f$  on the compact domain  $D$ .

Step 2: Uniform convergence condition

To prove that  $\text{Lin}_h$  converges uniformly to  $f$ , we must show that

$$\lim_{h \rightarrow \infty} \sup_{y \in D} |f(y) - \text{Lin}_h(y)| = 0.$$

In other words, the difference between the piecewise linear approximation and  $f$  must become arbitrarily small uniformly for all  $y \in D$  as  $h \rightarrow \infty$ .

The key to proving uniform convergence is to bound the error between  $\text{Lin}_h$  and  $f$  on each cell of the partition and show that the maximum error across all cells tends to zero as the mesh is refined.

The error estimate for piecewise linear interpolation of a differentiable function  $f(y_1, y_2, \dots, y_n)$  depends on the smoothness of the function and the size of the partition (mesh) used in the interpolation. Specifically, when we approximate  $f$  using piecewise linear functions, the error can be described in terms of the diameter of the regions in the partition and the second derivatives of  $f$  [4] as

$$|f(y) - \text{Lin}_{h,i}(y)| \leq \frac{1}{2} \|\nabla^2 f(\xi_{h,i})\| (\text{diam}(C_{h,i}))^2,$$

where  $\text{diam}(C_{h,i})$  is the diameter (the maximum distance between any two points) of the cell  $C_{h,i}$  and  $\nabla^2 f(\xi_{h,i})$  is the Hessian of  $f$  evaluated at the point  $\xi_{h,i}$  inside the cell.  $P_h$  be a partition of  $D$  into  $h$  regions, and  $\text{Lin}_h(y)$  be the corresponding piecewise linear interpolation. The global error for the entire domain can be bounded by considering the worst-case error over all the cells  $C_{h,i}$  in the partition. Since the error on each cell  $C_{h,i}$  depends on  $\text{diam}(C_{h,i})^2$ , we can sum the errors across all cells. If we refine the partition (i.e., make the cells smaller), the error in each cell decreases. The global error is controlled by the maximum diameter of the cells in the partition, so the total error can be bounded by

$$\sup_{y \in D} |f(y) - \text{Lin}_h(y)| \leq \frac{1}{2} \|\nabla^2 f(\xi)\| \cdot \max_{C_{h,i} \in P_h} (\text{diam}(C_{h,i}))^2.$$



Thus, the error estimate for piecewise linear interpolation of  $f(y_1, y_2, \dots, y_n)$  can be expressed as

$$|f(y) - \text{Lin}_h(y)| = O(\text{diam}(C_{h,i})^2),$$

where  $\text{diam}(C_{h,i})$  is the diameter of the cells in the partition and the constant hidden in the  $O(\cdot)$  notation depends on the smoothness of  $f$ , particularly the bounds on  $\|\nabla^2 f\|$  on  $D$ . If  $f$  is twice continuously differentiable, i.e.,  $f \in C^2(D \mapsto \mathbb{R}^n)$ , then Hessian matrix is bounded and symmetric on  $D$  and  $\|\nabla^2 f\|$  represents the largest absolute eigenvalue of  $\nabla^2 f$  on  $D$ .

**Definition 3.** A function  $\tilde{f} : \mathbb{R}^n \mapsto \mathbb{R}^n$  is globally Lipschitz continuous on  $\mathbb{R}^n$  if there exists a constant  $\tilde{L}$  such that

$$|\tilde{f}(x) - \tilde{f}(y)| \leq \tilde{L}|x - y|, \quad \forall x, y \in \mathbb{R}^n.$$

Here,  $|\cdot|$  denotes the Euclidean norm, and the smallest such  $\tilde{L}$  is called the Lipschitz constant of  $\tilde{f}(y)$ .

If the function  $\tilde{f} : \mathbb{R}^n \mapsto \mathbb{R}^n$  is continuously differentiable (i.e.,  $\tilde{f} \in C^1(\mathbb{R}^n)$ ), then a sufficient condition for  $\tilde{f}$  to be globally Lipschitz is that there exists a constant  $M > 0$  such that the norm of the Jacobian matrix of  $\tilde{f}$  is bounded, i.e.,

$$\|\nabla \tilde{f}(y)\| \leq M, \quad \forall y \in \mathbb{R}^n,$$

where  $\nabla \tilde{f}(y)$  is the Jacobian matrix of  $\tilde{f}$  at  $y$  and  $\|\nabla \tilde{f}(y)\|$  is the operator norm of the Jacobian which is defined as the largest singular value of the Jacobian matrix. This singular value corresponds to the square root of the largest eigenvalue of the matrix  $\nabla \tilde{f}(y)^T \nabla \tilde{f}(y)$ , where the superscript  $T$  denotes the transpose of the Jacobian matrix  $\nabla \tilde{f}(y)$ . If this condition is satisfied, then  $\tilde{f}$  is globally Lipschitz with Lipschitz constant  $\tilde{L} = M$  because of the mean value theorem.

Consider nonlinear system

$$y^{(n)}(t) + f(y(t), y'(t), \dots, y^{(n-1)}(t)) = u(t), \quad (2)$$

on the time interval  $[0, \infty)$  with the initial conditions

$$y(0) = y'(0) = \dots = y^{(n-1)}(0) = 0,$$

or reformulated as an equivalent system of first-order ordinary differential equations (ODEs) by introducing variables

$$y_1 = y, \quad y_2 = y', \quad \dots, \quad y_{n-1} = y^{(n-2)}, \quad y_n = y^{(n-1)}.$$

Then, the equation becomes

$$\left. \begin{array}{l} y_1' = y_2, \\ y_2' = y_3, \\ \vdots \\ y_{n-1}' = y_n, \\ y_n' = -f(y_1, y_2, \dots, y_n) + u(t) \end{array} \right\} \triangleq y' = \tilde{f}(y) + \tilde{u}(t). \quad (3)$$

The initial conditions become

$$y_1(0) = y_2(0) = \dots = y_n(0) = 0.$$

**Lemma 4.** *If  $f$  is globally Lipschitz with Lipschitz constant  $L$ , then also  $\tilde{f}$  is globally Lipschitz with Lipschitz constant  $\tilde{L} = (n - 1 + L^2)^{1/2}$ .*

PROOF. To prove that  $\tilde{f}$  is globally Lipschitz, we show that

$$|\tilde{f}(x) - \tilde{f}(y)| \leq \tilde{L}|x - y| \quad \text{for all } x, y \in \mathbb{R}^n,$$

where  $|\cdot|$  denotes the Euclidean norm.

Let  $x = [x_1, x_2, \dots, x_n]^\top$  and  $y = [y_1, y_2, \dots, y_n]^\top$ . Then,

$$\tilde{f}(x) - \tilde{f}(y) = \begin{bmatrix} x_2 - y_2 \\ x_3 - y_3 \\ \vdots \\ x_n - y_n \\ f(x) - f(y) \end{bmatrix}.$$

The Euclidean norm of this difference is

$$|\tilde{f}(x) - \tilde{f}(y)| = \sqrt{\sum_{i=2}^n (x_i - y_i)^2 + (f(x) - f(y))^2}.$$

The Euclidean norm of the input difference is

$$|x - y| = \sqrt{\sum_{i=1}^n (x_i - y_i)^2}.$$

Using the definition of Lipschitz continuity for  $f$ , we have  $|f(x) - f(y)| \leq L|x - y|$ . Substituting the Lipschitz bound for  $f$ ,

$$|\tilde{f}(x) - \tilde{f}(y)| \leq \sqrt{\sum_{i=2}^n (x_i - y_i)^2 + L^2|x - y|^2}.$$

Separating  $|x - y|^2$  into its components

$$|x - y|^2 = (x_1 - y_1)^2 + \sum_{i=2}^n (x_i - y_i)^2.$$

Therefore,

$$|\tilde{f}(x) - \tilde{f}(y)| \leq \sqrt{|x - y|^2 - (x_1 - y_1)^2 + L^2|x - y|^2}.$$

Factoring  $|x - y|^2$  yields

$$|\tilde{f}(x) - \tilde{f}(y)| \leq \sqrt{|x - y|^2 \left(1 - \frac{(x_1 - y_1)^2}{|x - y|^2} + L^2\right)} \leq \left(\sqrt{1 - \frac{(x_1 - y_1)^2}{|x - y|^2} + L^2}\right) |x - y|.$$

Maximizing the coefficient inside the square root gives the Lipschitz constant for  $\tilde{f}$ ,

$$\tilde{L} = \sqrt{(n - 1) + L^2}.$$

#### 4. Lipschitz Constant of the Piecewise Linear Approximation $\text{Lin}_h(\mathbf{y})$

To prove that the Lipschitz constant  $L_{\text{pwl}}$  of the piecewise linear approximation of a function  $f(y) : \mathbb{R}^n \mapsto \mathbb{R}$  satisfies  $L_{\text{pwl},h} \leq L$ , we will proceed as follows. A function  $f(y)$  is globally Lipschitz if there exists a constant  $L \geq 0$  such that

$$|f(x) - f(y)| \leq L|x - y|, \quad \forall x, y \in \mathbb{R}^n.$$

A piecewise linear approximation of  $f(y)$  is constructed by partitioning the compact domain  $D \subset \mathbb{R}^n$  into a set of non-overlapping cells  $\{C_{h,i}, i =$

$1, 2, \dots, h\}$ . Within each region  $C_{h,i}$ , the function is approximated as a linear function  $\text{Lin}_{h,i}(y)$ , so

$$f(y) \approx \text{Lin}_{h,i}(y), \quad y \in C_{h,i}.$$

For simplicity, assume that the piecewise linear approximation is exact at the vertices of the simplex and  $\text{Lin}_{h,i}(y)$  is defined as

$$\text{Lin}_{h,i}(y) = a_{h,i}y + b_{h,i},$$

where  $a_{h,i} \in \mathbb{R}^n$  is the gradient (or slope vector) of the linear function in region  $C_{h,i}$ .

For future reference, we introduce cumulative notation analogous to (1):

$$a_h \triangleq \{a_{h,i} \mid i = 1, 2, \dots, h\}$$

and

$$b_h \triangleq \{b_{h,i} \mid i = 1, 2, \dots, h\}.$$

This notation will be used to collectively represent the sequences of coefficients  $\{a_{h,i}\}$  and  $\{b_{h,i}\}$  for  $i = 1, 2, \dots, h$ .

The Lipschitz constant  $L_{\text{pwl}}$  of the piecewise linear approximation is defined as

$$L_{\text{pwl},h} = \sup_{x,y \in D, x \neq y} \frac{|\text{Lin}_{h,i}(x) - \text{Lin}_{h,i}(y)|}{|x - y|}.$$

Within a single region  $C_{h,i}$ , since  $\text{Lin}_{h,i}(y)$  is linear, its Lipschitz constant is given by  $L_{h,i} = |a_{h,i}|$ , where  $|a_{h,i}|$  is the norm of the gradient vector  $a_{h,i}$  of  $\text{Lin}_{h,i}(y)$ . The global Lipschitz constant of the piecewise linear approximation is

$$L_{\text{pwl},h} = \max_{i=1,2,\dots,h} L_{h,i} = \max_{i=1,2,\dots,h} |a_{h,i}|.$$

Each linear function  $\text{Lin}_{h,i}(y)$  is constructed to approximate  $f(y)$  within cell  $C_{h,i}$ . Typically  $\text{Lin}_{h,i}(y)$  matches  $f(y)$  exactly at the vertices of  $C_{h,i}$ . For example, in simplicial interpolation, the gradient is derived from the values of  $f(y)$  at the vertices. Since  $f(y)$  is Lipschitz continuous with constant  $L$ , the gradient  $a_{h,i}$  of  $\text{Lin}_{h,i}(y)$  within  $C_{h,i}$  is derived from  $f(y)$ . Specifically,  $|a_{h,i}|$  reflects the "local slope" of  $f(y)$  within  $C_{h,i}$ . Since  $f(y)$  is Lipschitz continuous with constant  $L$ , the maximum rate of change of  $f(y)$  is bounded by  $L$ , i.e.

$$|\nabla f(y)| \leq L, \quad \forall y \in \mathbb{R}^n.$$

Because  $\text{Lin}_{h,i}(y)$  is constructed to approximate  $f(y)$  and its gradient  $a_{h,i}$  is derived from  $f(y)$ , we have

$$|a_{h,i}| \leq L, \quad i = 1, 2, \dots, h.$$

The global Lipschitz constant of the piecewise linear approximation is the maximum gradient norm across all regions

$$L_{\text{pwl},h} = \max_{i=1,2,\dots,h} |a_{h,i}| \leq L.$$

To analyze the behavior of  $a_{h,i}$  (the gradient of the piecewise linear approximation) as  $h \rightarrow \infty$ , we must consider how the partition of the domain  $\mathbb{R}^n$  evolves and how the approximation behaves as the number of regions  $C_{h,i}$  increases. Since the piecewise linear approximation is exact at the vertices of the simplex,  $f(y) = \text{Lin}_{h,i}(y)$  at these points. This ensures that as  $h \rightarrow \infty$ , the approximation becomes finer and better represents  $f(y)$ . Each  $a_{h,i}$  represents the slope of the linear approximation  $\text{Lin}_{h,i}(y)$  within region  $C_{h,i}$ , and it is determined by the values of  $f(y)$  at the vertices of  $C_{h,i}$ . Specifically,  $a_{h,i}$  approximates the gradient of  $f(y)$  over  $C_{h,i}$ . As  $h \rightarrow \infty$ , the regions  $C_{h,i}$  become arbitrarily small, effectively shrinking to points. Within each region  $C_{h,i}$ , the gradient  $a_{h,i}$  approximates the gradient,  $\nabla f(y)$ , over that region, under assumption that  $f(y) = f(y_1, y_2, \dots, y_n)$  is at least differentiable in  $D$ .

## 5. Existence and uniqueness of a solution for nonlinear system

In this section, we formulate and prove the main results regarding the existence and uniqueness of the solution to the nonlinear system (2) with a zero initial conditions. To achieve this, we employ a specially chosen weighted sup-norm, which ensures that the Laplace transform can be applied to the system. Subsequently, this approach allows us to formally define the transfer function of the nonlinear system as the limiting case of its piecewise linearization. This, in turn, facilitates the standard analysis of the system using transfer function algebra within a closed-loop control framework.

**Theorem 5.** *Let  $f \in C^2(\mathbb{R}^n \mapsto \mathbb{R})$  is globally Lipschitz in  $(y, y', \dots, y^{(n-1)})$  with Lipschitz constant  $L$  and  $u \in C(\mathbb{R} \mapsto \mathbb{R})$ . Then the initial value problem*

$$y^{(n)} + f(y, y', \dots, y^{(n-1)}) = u(t),$$

on  $[0, \infty)$  with a zero initial conditions

$$y(0) = y'(0) = \dots = y^{(n-1)}(0) = 0,$$

has a unique solution  $y(t)$  defined on  $\mathbb{R}$  satisfying here the inequality

$$|y(t)| \leq Ke^{2\tilde{L}|t|}, \quad K \geq 0, \quad \tilde{L} = (n - 1 + L^2)^{1/2}.$$

PROOF. The  $n$ -th order differential equation can be reformulated as a system of first-order ODEs (3).

Define on the space  $C(\mathbb{R} \mapsto \mathbb{R}^n)$  of continuous functions the weighted sup-norm

$$\|y(t)\|_{\tilde{L}} = \sup_{t \in \mathbb{R}} e^{-2\tilde{L}|t|} |y(t)|$$

and consider the space of continuous functions that have a finite norm with this formula. This space contains the constant functions.

Then the Picard operator  $(P(y))(t)$  with zero initial conditions is defined as

$$(P(y))(t) = \int_0^t (\tilde{f}(y(\tau)) + u(\tau)) d\tau,$$

where  $\tilde{f}$  is a Lipschitz function with Lipschitz constant  $\tilde{L} > 0$ . This means

$$|\tilde{f}(x) - \tilde{f}(y)| \leq \tilde{L}|x - y|, \quad \forall x, y \in \mathbb{R}^n.$$

To prove that  $(P(y))(t)$  is contractive, we show that the mapping  $P : y(t) \mapsto (P(y))(t)$  satisfies the contraction condition i.e., there exists  $0 \leq k < 1$  such that

$$\|(P(x))(t) - (P(y))(t)\|_{\tilde{L}} \leq k\|x(t) - y(t)\|_{\tilde{L}},$$

By definition

$$(P(x))(t) - (P(y))(t) = \int_0^t (\tilde{f}(x(\tau)) - \tilde{f}(y(\tau))) d\tau.$$

The weighted sup-norm is given by

$$\|P(x) - P(y)\|_{\tilde{L}} = \sup_{t \in \mathbb{R}} e^{-2\tilde{L}|t|} \left| \int_0^t (\tilde{f}(x(\tau)) - \tilde{f}(y(\tau))) d\tau \right|.$$

By the Lipschitz condition on  $\tilde{f}$ ,

$$|\tilde{f}(x(\tau)) - \tilde{f}(y(\tau))| \leq \tilde{L}|x(\tau) - y(\tau)|.$$

This implies

$$\left| \int_0^t (\tilde{f}(x(\tau)) - \tilde{f}(y(\tau))) d\tau \right| \leq \int_0^t \tilde{L} |x(\tau) - y(\tau)| d\tau.$$

Using the definition of the weighted sup-norm  $\|\cdot\|_{\tilde{L}}$ ,

$$|x(\tau) - y(\tau)| \leq e^{2\tilde{L}|\tau|} \|x - y\|_{\tilde{L}}.$$

Substitute this bound into the integral

$$\left| \int_0^t (\tilde{f}(x(\tau)) - \tilde{f}(y(\tau))) d\tau \right| \leq \int_0^t \tilde{L} e^{2\tilde{L}|\tau|} \|x - y\|_{\tilde{L}} d\tau.$$

Now, consider the weighted sup-norm with the factor  $e^{-2\tilde{L}|t|}$

$$e^{-2\tilde{L}|t|} \left| \int_0^t (\tilde{f}(x(\tau)) - \tilde{f}(y(\tau))) d\tau \right| \leq e^{-2\tilde{L}|t|} \int_0^t \tilde{L} e^{2\tilde{L}|\tau|} \|x - y\|_{\tilde{L}} d\tau.$$

For  $\tau \in [0, t]$ , we have  $|\tau| = \tau$  (since  $\tau \geq 0$ ). Thus,

$$e^{-2\tilde{L}|t|} e^{2\tilde{L}|\tau|} = e^{-2\tilde{L}(t-\tau)}.$$

This gives

$$e^{-2\tilde{L}|t|} \left| \int_0^t (\tilde{f}(x(\tau)) - \tilde{f}(y(\tau))) d\tau \right| \leq \int_0^t \tilde{L} e^{-2\tilde{L}(t-\tau)} \|x - y\|_{\tilde{L}} d\tau.$$

The factor  $e^{-2\tilde{L}(t-\tau)}$  integrates to a finite value

$$\int_0^t e^{-2\tilde{L}(t-\tau)} d\tau = \frac{1 - e^{-2\tilde{L}t}}{2\tilde{L}} \leq \frac{1}{2\tilde{L}}.$$

Thus

$$e^{-2\tilde{L}|t|} \left| \int_0^t (\tilde{f}(x(\tau)) - \tilde{f}(y(\tau))) d\tau \right| \leq \frac{\tilde{L}}{2\tilde{L}} \|x - y\|_{\tilde{L}} = \frac{1}{2} \|x - y\|_{\tilde{L}}.$$

For  $t < 0$ , the proof works almost exactly the same with slight adjustments due to the sign of  $t$ . These adjustments primarily involve handling the integration limits and ensuring the correct behavior of the exponential weighting factor  $e^{-2\tilde{L}|t|}$ , but the underlying steps and reasoning remain identical.

Taking the supremum over  $t \in \mathbb{R}$ , we obtain

$$\|P(x) - P(y)\|_{\tilde{\mathcal{L}}} \leq \frac{1}{2} \|x - y\|_{\tilde{\mathcal{L}}}.$$

Since  $\frac{1}{2} < 1$ , the operator  $P$  is a contraction.

To apply the Banach Fixed-Point Theorem, we need to verify that the Picard operator  $P(y)$  maps the chosen function space into itself. Specifically, we must show that if  $y(t)$  belongs to the space of continuous functions equipped with the weighted sup-norm  $\|y(t)\|_{\tilde{\mathcal{L}}} = \sup_{t \in \mathbb{R}} e^{-2\tilde{L}|t|} |y(t)| < \infty$ , then  $P(y)(t)$  also belongs to the same space.

Define the space  $\mathcal{C}_{\tilde{\mathcal{L}}}$  as

$$\mathcal{C}_{\tilde{\mathcal{L}}} = \{y \in C(\mathbb{R} \mapsto \mathbb{R}^n) : \|y\|_{\tilde{\mathcal{L}}} < \infty\}.$$

A function  $y(t) \in \mathcal{C}_{\tilde{\mathcal{L}}}$  satisfies

$$\|y\|_{\tilde{\mathcal{L}}} = \sup_{t \in \mathbb{R}} e^{-2\tilde{L}|t|} |y(t)| < \infty.$$

This implies that for all  $t \in \mathbb{R}$ ,

$$|y(t)| \leq K e^{2\tilde{L}|t|},$$

where  $K = \|y\|_{\tilde{\mathcal{L}}}$  is a finite constant.

Recall that the Picard operator is defined as

$$(P(y))(t) = \int_0^t (\tilde{f}(y(\tau)) + \tilde{u}(\tau)) d\tau,$$

where  $\tilde{f}$  satisfies the Lipschitz condition with constant  $\tilde{L} > 0$ , and  $\tilde{u}(t) \in \mathcal{C}_{\tilde{\mathcal{L}}}$  is a continuous input. We want to prove that

$$\text{If } y \in \mathcal{C}_{\tilde{\mathcal{L}}}, \text{ then } P(y) \in \mathcal{C}_{\tilde{\mathcal{L}}}.$$

The operator  $P(y)$  involves the integral

$$(P(y))(t) = \int_0^t (\tilde{f}(y(\tau)) + \tilde{u}(\tau)) d\tau.$$

Since  $y \in \mathcal{C}_{\tilde{\mathcal{L}}}$ , it follows that  $\|\tilde{f}(y)\|_{\tilde{\mathcal{L}}} < \infty$  because  $\tilde{f}$  is Lipschitz, and so  $\|\tilde{f}(y)\|_{\tilde{\mathcal{L}}} \leq |\tilde{f}(0)| + \tilde{L}\|y\|_{\tilde{\mathcal{L}}}$ . Additionally,  $u(t) \in \mathcal{C}_{\tilde{\mathcal{L}}}$  is continuous and



$\|\tilde{u}\|_{\tilde{L}} < \infty$ . Thus, the integrand  $\tilde{f}(y(\tau)) + \tilde{u}(\tau)$  is well-defined and integrable for all  $t \in \mathbb{R}$ . We need to show

$$\|P(y)\|_{\tilde{L}} = \sup_{t \in \mathbb{R}} e^{-2\tilde{L}|t|} \left| \int_0^t (\tilde{f}(y(\tau)) + \tilde{u}(\tau)) d\tau \right| < \infty.$$

Using the triangle inequality

$$\left| \int_0^t (\tilde{f}(y(\tau)) + \tilde{u}(\tau)) d\tau \right| \leq \int_0^t |\tilde{f}(y(\tau))| d\tau + \int_0^t |\tilde{u}(\tau)| d\tau.$$

After applying the weighted sup-norm, we have

$$e^{-2\tilde{L}|t|} \left| \int_0^t (\tilde{f}(y(\tau)) + \tilde{u}(\tau)) d\tau \right| \leq e^{-2\tilde{L}|t|} \int_0^t e^{2\tilde{L}|\tau|} \|\tilde{f}(y)\|_{\tilde{L}} d\tau + e^{-2\tilde{L}|t|} \int_0^t e^{2\tilde{L}|\tau|} \|\tilde{u}\|_{\tilde{L}} d\tau.$$

Then

$$e^{-2\tilde{L}|t|} \left| \int_0^t (\tilde{f}(y(\tau)) + \tilde{u}(\tau)) d\tau \right| \leq \|\tilde{f}(y)\|_{\tilde{L}} \cdot \frac{1}{2\tilde{L}} (1 - e^{-2\tilde{L}|t|}) + \|\tilde{u}\|_{\tilde{L}} \cdot \frac{1}{2\tilde{L}} (1 - e^{-2\tilde{L}|t|}).$$

Taking the supremum over  $t \in \mathbb{R}$ , we find that the weighted sup-norm remains finite

$$\|P(y)\|_{\tilde{L}} \leq \frac{\|\tilde{f}(y)\|_{\tilde{L}} + \|\tilde{u}\|_{\tilde{L}}}{2\tilde{L}} < \infty.$$

**Remark 1.** The Laplace transform of  $y(t)$  defined as

$$\mathcal{L}_-[y(t)] = \int_{0^-}^{\infty} y(t) e^{-st} dt,$$

where  $s \in \mathbb{C}$  with  $\Re(s) = \sigma > 0$  is well-defined for all functions  $y(t) \in \mathcal{C}_{\tilde{L}}$  provided  $\Re(s) = \sigma > 2\tilde{L}$ . This condition ensures that the exponential decay induced by  $e^{-\sigma t}$  dominates any growth in  $y(t)$ , making the integral converge.

In the definition, here  $t = 0^-$  refers to the limit where  $t$  approaches 0 from the left-hand side, capturing pre-initial values of the function  $y(t)$ . This definition enables the analysis of functions that may exhibit discontinuities or impulsive behavior, such as those involving the Dirac delta  $\delta(t)$  and its derivative.

This definition of the Laplace transform implies the time-derivative rule

$$\mathcal{L}_-[y'(t)] = sY(s) - y(0^-),$$

whereby initial conditions existing before  $t = 0$  are brought into the analysis. This formulation ensures that the Laplace transform correctly incorporates the effects of any discontinuities at  $t = 0$ .

For higher derivatives, the rule generalizes as

$$\mathcal{L}_-[y^{(n)}(t)] = s^n Y(s) - s^{n-1}y(0^-) - \dots - y^{(n-1)}(0^-).$$

Zero initial conditions

$$y(0) = y'(0) = \dots = y^{(n-1)}(0) = 0,$$

when using the Laplace transform, will be understood in the sense of

$$y(0^-) = y'(0^-) = \dots = y^{(n-1)}(0^-) = 0.$$

The initial-value theorem states that

$$\lim_{s \rightarrow \infty \cdot 1} sY(s) = y(0^+), \quad (4)$$

where  $s \rightarrow \infty \cdot 1$  indicates that the limit is taken along the positive real axis. This theorem is particularly useful for validating solutions of differential equations and determining the immediate response of a system to initial conditions. An excellent and inspiring discussion on the topic of the Laplace transform can be found in the paper [10].

In the context of solving linear differential equations using the Laplace transform, the pre-initial values  $y(0^-)$ ,  $y'(0^-)$ ,  $\dots$  plays a critical role in converting the problem into the Laplace domain. By incorporating both pre-initial and post-initial values, this approach ensures that discontinuities in  $y(t)$  or its derivatives are properly handled and impulsive inputs such as  $\delta(t)$  or  $\delta'(t)$  are accurately incorporated into the solution.

## 6. Convergence of the solution of the piecewise linear approximation to the solution of the original nonlinear system

Consider the infinite sequence of piecewise linear approximation of original nonlinear system (2)

$$y_h^{(n)}(t) + \text{Lin}_h(\bar{y}_h(t)) = u_h(t), \quad t \geq 0 \quad (5)$$

with zero initial conditions

$$y_h(0) = y_h'(0) = \dots = y_h^{(n-1)}(0) = 0,$$

where  $\bar{y}_h(t) = (y_h(t), y'_h(t), \dots, y_h^{(n-1)}(t))$ , and  $\{h\}$  is an infinite and increasing sequence of natural numbers, given that  $u_h(t) \rightarrow u(t)$  uniformly on every interval  $[0, T] \subset \mathbb{R}$ ,  $\text{Lin}_h(y)$  is globally Lipschitz with constant  $L$ , and  $u_h, u \in \mathcal{C}_{\tilde{L}}$ . Analogously as in (3), for equivalent first order system we use notation

$$y'_h = \tilde{\text{Lin}}_h(y_h) + \tilde{u}_h(t) \quad (6)$$

As has been proven before  $\tilde{\text{Lin}}_h(y) \in \mathcal{C}_{\tilde{L}}$ ,  $\text{Lin}_h(y)$  to  $f(y)$  uniformly on any compact domain  $D \subset \mathbb{R}^n$  if  $f$  is twice continuously differentiable and  $\text{Lin}_h(y)$  is globally Lipschitz with the same constant as  $f(y)$ .

Thus, for any compact set  $D \subset \mathbb{R}^n$  and any  $\epsilon_f > 0$ , there exists  $h_0$  such that for all  $h \geq h_0$

$$\sup_{y \in D} |\text{Lin}_h(y) - f(y)| < \epsilon_f.$$

To study the relationship between  $y_h(t)$  and  $y(t)$ , define the difference

$$z_h(t) = y_h(t) - y(t).$$

Subtract the equations (6) and (3) we have

$$\frac{dz_h}{dt} = [\tilde{\text{Lin}}_h(y_h) - \tilde{f}(y)] + [\tilde{u}_h(t) - \tilde{u}(t)].$$

Using the triangle inequality

$$|\tilde{\text{Lin}}_h(y_h) - \tilde{f}(y)| \leq |\tilde{\text{Lin}}_h(y_h) - \tilde{\text{Lin}}_h(y)| + |\tilde{\text{Lin}}_h(y) - \tilde{f}(y)|.$$

The term  $|\tilde{\text{Lin}}_h(y_h) - \tilde{\text{Lin}}_h(y)|$  depends on the Lipschitz continuity of  $\tilde{\text{Lin}}_h$

$$|\tilde{\text{Lin}}_h(y_h) - \tilde{\text{Lin}}_h(y)| \leq \tilde{L}_h |y_h - y| = \tilde{L}_h |z_h|,$$

where  $\tilde{L}_h$  is the Lipschitz constant for  $\tilde{\text{Lin}}_h(y)$ . For large  $h$ ,  $\tilde{L}_h$  can be bounded by a common Lipschitz constant  $\tilde{L}$  for  $\tilde{f}(y)$ , due to uniform convergence. The term  $|\tilde{\text{Lin}}_h(y) - \tilde{f}(y)|$  depends on the uniform convergence of  $\tilde{\text{Lin}}_h(y) \rightarrow \tilde{f}(y)$ . On any compact  $D$ , this term can be made arbitrarily small by choosing  $h$  sufficiently large. Thus

$$\left| \frac{dz_h(t)}{dt} \right| \leq \tilde{L} |z_h(t)| + (\epsilon_f + \epsilon_u),$$

where  $\epsilon_f > 0$  and  $\epsilon_u > 0$  accounts for the uniform convergence error  $|\text{Lin}_h(y) - \tilde{f}(y)|$  on  $D$  and  $|\tilde{u}_h(t) - \tilde{u}(t)|$  on  $[0, T]$ , respectively. Using the inequality

$$\frac{d}{dt}|z_h(t)| \leq \left| \frac{d}{dt}|z_h(t)| \right| \leq \left| \frac{d}{dt}z_h(t) \right|$$

and Gronwall's inequality (Theorem 2), we can bound  $|z_h(t)|$

$$|z_h(t)| \leq (\epsilon_f + \epsilon_u) \frac{e^{\tilde{L}t} - 1}{\tilde{L}}.$$

For any fixed  $T$  and given  $(\epsilon_f + \epsilon_u) > 0$ , there exists  $h_0$  such that  $h \geq h_0$  ensures  $|z_h(t)|$  is arbitrarily small. This implies uniform convergence of  $y_h(t) \rightarrow y(t)$  on the finite interval  $[0, T]$ . We have just proven the following theorem.

**Theorem 6.** *Consider the infinite sequence of piecewise linear approximations of the original nonlinear system (2),*

$$y_h^{(n)}(t) + \text{Lin}_h(\bar{y}_h(t)) = u_h(t), \quad t \geq 0,$$

with zero initial conditions

$$y_h(0) = y_h'(0) = \dots = y_h^{(n-1)}(0) = 0,$$

where  $\bar{y}_h(t) = (y_h(t), y_h'(t), \dots, y_h^{(n-1)}(t))$ , and  $\{h\}$  is an infinite, increasing sequence of natural numbers. Assume that

1.  $u_h(t) \rightarrow u(t)$  uniformly on any finite interval  $[0, T] \subset \mathbb{R}$ ,
2.  $\text{Lin}_h(y)$  is globally Lipschitz with constant  $L$ , and
3.  $u_h(t), u(t) \in \mathcal{C}_{\tilde{L}}$ .

Additionally, let  $\text{Lin}_h(y) \rightarrow f(y)$  uniformly on any compact domain  $D \subset \mathbb{R}^n$ , and let  $f(y)$  be twice continuously differentiable and globally Lipschitz. Then, for any compact  $D \subset \mathbb{R}^n$  and finite  $T > 0$ , the solution  $y_h(t)$  of the piecewise linearized system converges uniformly to the solution  $y(t)$  of the original nonlinear system as  $h \rightarrow \infty$ :

$$\sup_{t \in [0, T]} |y_h(t) - y(t)| \rightarrow 0.$$

## 7. Definition of transfer function for nonlinear system

We are considering the piecewise linear approximation of the original system. For the system described by Equation (5)

$$y_h^{(n)}(t) + \text{Lin}_h(\bar{y}_h(t)) = u_h(t), \quad t \geq 0,$$

we define the equivalent first-order system

$$y_h' = \tilde{\text{Lin}}_h(y_h) + \tilde{u}_h(t),$$

where  $y_h \in \mathbb{R}^n$ ,  $\text{Lin}_h(y)$  is globally Lipschitz, and  $\tilde{\text{Lin}}_h(y)$  represents the first-order equivalent formulation of  $\text{Lin}_h(y)$ .

Taking the Laplace transform of both sides (with zero initial conditions  $y_h(0) = y_h'(0) = \dots = y_h^{(n-1)}(0) = 0$ ), we get

$$\mathcal{L}_-[y_h^{(n)}(t)] + \mathcal{L}_-[\text{Lin}_h(\bar{y}_h(t))] = \mathcal{L}_-[u_h(t)].$$

Using standard Laplace transform properties

$$\mathcal{L}_-[y_h^{(n)}(t)] = s^n Y_h(s),$$

where  $Y_h(s)$  is the Laplace transform of  $y_h(t)$ . Substituting, we have

$$s^n Y_h(s) + \mathcal{L}_-[\text{Lin}_h(\bar{y}_h(t))] = U_h(s),$$

where  $U_h(s) = \mathcal{L}_-[u_h(t)]$ .

If  $\text{Lin}_h(\bar{y}_h) = a_h y_h + b_h$ , where  $a_h$  is the cumulative gradient of the linear function in compact domain  $D$ , its Laplace transform becomes

$$\mathcal{L}_-[\text{Lin}_h(\bar{y}_h)] = a_h \cdot (1, s, \dots, s^{n-1}) Y_h(s) + \mathcal{L}_-[b_h].$$

Substituting, we have

$$s^n Y_h(s) + a_h \cdot (1, s, \dots, s^{n-1}) Y_h(s) + \frac{b_h}{s} = U_h(s).$$

Reorganizing the equation,

$$(s^n + a_h \cdot (1, s, \dots, s^{n-1})) Y_h(s) = U_h(s) - \frac{b_h}{s}.$$

Thus, the solution becomes

$$Y_h(s) = \frac{1}{(s^n + a_h \cdot (1, s, \dots, s^{n-1}))} \left( U_h(s) - \frac{b_h}{s} \right)$$

and the transfer function  $G_h(s)$  of the system is

$$G_h(s) = \frac{1}{s^n + a_h \cdot (1, s, \dots, s^{n-1})},$$

where  $\cdot$  stands for the standard dot product. However, the input now includes a term due to  $b_h$

$$Y_h(s) = G_h(s)U_h(s) - G_h(s)\frac{b_h}{s}.$$

The transfer function describes the relationship between the input  $u_h(t)$  and the output  $y_h(t)$  in the Laplace domain. For piecewise linear systems,  $G_h(s)$  may vary across different regions  $C_{h,i}$ , depending on the coefficients  $a_{h,i}$  and  $b_{h,i}$ .

As  $h \rightarrow \infty$ , the piecewise linear approximations  $\text{Lin}_h(\bar{y}_h)$  converge uniformly to the nonlinear function  $f(y)$  on compact domains. Similarly,  $u_h(t) \rightarrow u(t)$  uniformly on any interval  $[0, T]$ . Therefore, as  $h \rightarrow \infty$ , the solution  $y_h(t)$  to the linear system converges uniformly to the solution  $y(t)$  of the original nonlinear system  $y^{(n)}(t) + f(\bar{y}(t)) = u(t)$ . For this system, we cannot directly define a transfer function due to the nonlinearity of  $f(y)$ . However, in the limit of piecewise linearized regime, the transfer function takes the form

$$G(s) = \frac{1}{s^n + \nabla f(y) \cdot (1, s, \dots, s^{n-1})}. \quad (7)$$

Here,  $\nabla f(y)$  represents the gradient of  $f(y) = f(y_1, y_2, \dots, y_n)$  at the operating point  $y \in D \subset \mathbb{R}^n$ .

Consider a feedback control system, as depicted schematically in Figure 1,

$$\begin{aligned} Y_h(s) &= G_h(s)U_h(s) - G_h(s)\frac{b_h}{s}, \\ U_h(s) &= C_h(s)E_h(s), \\ E_h(s) &= R(s) - Y_h(s). \end{aligned}$$

The closed-loop system equation is given as

$$(1 + C_h(s)G_h(s))Y_h(s) = C_h(s)G_h(s)R(s) - G_h(s)\frac{b_h}{s},$$

where

$C_h(s) = K_{p,h} + \frac{K_{i,h}}{s} + K_{d,h}s$  is the transfer function of the PID controller,  
 $G_h(s)$  is the plant's piecewise linearization transfer function,  
 $R(s) = \frac{1}{s}$  is the Laplace transform of a unit step input,  
 $b_h$  acts like a source of persistent input that does not decay (if  $b_h \neq 0$ ).  
 Substituting  $G_h(s), C_h(s)$  and  $R(s)$  we obtain

$$\begin{aligned} & \left( s^n + a_h \cdot (1, s, \dots, s^{n-1}) + K_{p,h} + \frac{K_{i,h}}{s} + K_{d,h}s \right) Y_h(s) \\ &= \left( K_{p,h} + \frac{K_{i,h}}{s} + K_{d,h}s \right) \frac{1}{s} - \frac{b_h}{s} \end{aligned}$$

Now multiply through by  $s$  to clear the denominators

$$\begin{aligned} & (s^{n+1} + a_h \cdot (s, s^2, \dots, s^n) + K_{p,h}s + K_{i,h} + K_{d,h}s^2) Y_h(s) \\ &= K_{p,h}s + \frac{K_{i,h}}{s} + K_{d,h}s^2 - b_h. \end{aligned}$$

In a form of differential equation in the time domain under zero initial conditions when applying the inverse Laplace transform, each term on the left-hand side corresponds to derivatives of  $y_h(t)$ :

$s^{n+1}Y_h(s)$  corresponds to the  $(n+1)$ -th derivative of  $y_h(t)$ , written as  $y_h^{(n+1)}(t)$ ,

$a_h \cdot (s, s^2, \dots, s^n)Y_h(s)$  gives terms up to the  $n$ -th derivative of  $y_h(t)$ , namely  $a_h \cdot (y_h'(t), y_h''(t), \dots, y_h^{(n)}(t))$ ,

$K_{p,h}sY_h(s)$  corresponds to  $K_{p,h}y_h'(t)$ ,

$K_{d,h}s^2Y_h(s)$  corresponds to  $K_{d,h}y_h''(t)$ ,

$K_{i,h}Y_h(s)$  corresponds to  $K_{i,h}y_h(t)$  directly.

Thus, the left-hand side in the time domain becomes

$$y_h^{(n+1)}(t) + a_h \cdot (y_h'(t), y_h''(t), \dots, y_h^{(n)}(t)) + K_{p,h}y_h'(t) + K_{i,h}y_h(t) + K_{d,h}y_h''(t).$$

The right-hand side is

$$K_{p,h} + \frac{K_{i,h}}{s} + K_{d,h}s - b_h.$$

Taking the inverse Laplace transform term by term:

$K_{p,h}$  corresponds to  $K_{p,h}\delta(t)$  (a Dirac delta),

$\frac{K_{i,h}}{s}$  corresponds to  $K_{i,h}\eta(t)$ , where  $\eta(t)$  is the unit step function,  
 $K_{d,h}s$  corresponds to  $K_{d,h}\delta'(t)$  (a Dirac doublet, i.e., the first derivative of the Dirac delta),  
 $b_h$  corresponds to  $b_h\delta(t)$ .

It follows from the general rule for the Laplace transform of the  $n$ -th derivative of the Dirac delta  $\delta^{(n)}(t)$  that

$$\mathcal{L}_-[\delta^{(n)}(t)] = s^n,$$

where the equality is understood in the sense of distributions [13], see also [10]. So the right-hand side in the time domain is

$$(K_{p,h} - b_h) \delta(t) + K_{i,h}\eta(t) + K_{d,h}\delta'(t).$$

Now, putting it all together, we get the following time-domain differential equation

$$\begin{aligned} y_h^{(n+1)}(t) + a_h \cdot (y_h'(t), y_h''(t), \dots, y_h^{(n)}(t)) + K_{p,h}y_h'(t) + K_{i,h}y_h(t) + K_{d,h}y_h''(t) \\ = (K_{p,h} - b_h) \delta(t) + K_{i,h}\eta(t) + K_{d,h}\delta'(t). \end{aligned} \quad (8)$$

The left-hand side is the dynamics of the linearized system under the PID controller. The right-hand side includes impulsive contributions  $\delta(t)$ ,  $\delta'(t)$  from the proportional and derivative control action and the persistent input  $K_{i,h}\eta(t)$ .

Let us consider the special case when  $n = 1$ . The time-domain differential equation (8) becomes

$$\begin{aligned} (1+K_{d,h})y_h''(t) + (a_h + K_{p,h})y_h'(t) + K_{i,h}y_h(t) \\ = (K_{p,h} - b_h) \delta(t) + K_{i,h}\eta(t) + K_{d,h}\delta'(t), \end{aligned} \quad (9)$$

$$y_h(0) = y_h'(0) = 0 \quad (10)$$

The assumptions about  $f$  being  $C^2(\mathbb{R} \mapsto \mathbb{R})$  with a globally bounded first derivative are sufficient for the convergence of the solutions  $y_h(t)$  to the solution  $y(t)$  of the nonlinear system  $y'(t) + f(y(t)) = u(t)$  as  $h \rightarrow \infty$ . If the piecewise linear approximations of nonlinear functions (as in the case of the piecewise linear models for nonlinear systems) converge uniformly, the interchange of limit and Laplace transform ensures that the analysis remains valid, as shown in Figure 2.

This is crucial when analyzing the behavior of systems in the frequency domain, as it ensures that we can rely on the Laplace transforms of the approximated models to obtain the results for the original system.



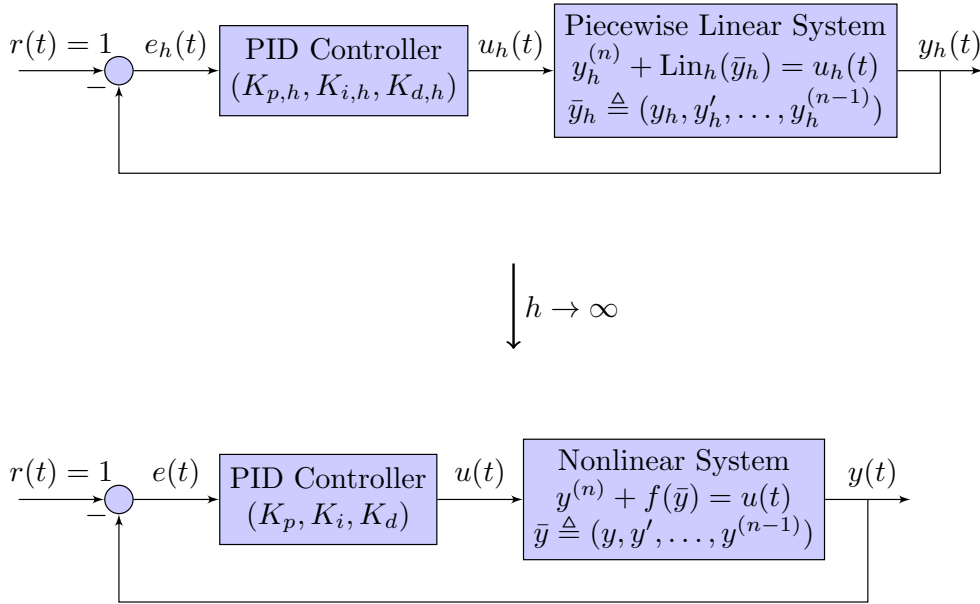


Figure 2: Convergence of piecewise linear approximation to the original nonlinear control system.

## 8. Numerical simulations

In this section, we will focus on numerical simulations to demonstrate the effectiveness of the described method based on the piecewise linearization of nonlinear systems. Both simulations will involve first-order systems, and in the simulations, we will use model (9), (10) which directly incorporates the zero initial state into the output response, while simultaneously avoiding issues caused by jump and impulse discontinuities on the right-hand side of the differential equation through the approximation of the impulsive functions  $\delta(t)$  and  $\delta'(t)$ . This is related to Remark 3.

To approximate the Dirac delta "function" and its derivative (the Dirac doublet), we will use the Gaussian function

$$\delta(t) \approx \frac{1}{\sigma\sqrt{2\pi}} e^{-\frac{t^2}{2\sigma^2}},$$

where  $\sigma$  is a small positive value that controls the width of the Gaussian peak. As  $\sigma$  becomes smaller, the Gaussian function becomes more sharply peaked at  $t = 0$ , and its integral over all time approaches 1, mimicking the

behavior of the Dirac delta. To approximate the Dirac doublet  $\delta'(t)$ , you would differentiate the Gaussian approximation of  $\delta(t)$ . The derivative of the Gaussian function with respect to  $t$  is

$$\delta'(t) \approx -\frac{t}{\sigma^2} \cdot \frac{1}{\sigma\sqrt{2\pi}} e^{-\frac{t^2}{2\sigma^2}},$$

where  $\sigma$  is again a small positive value that controls the width of the Gaussian peak.

Dirac doublet  $\delta'(t)$  is a distribution that behaves like a pulse with a singularity at  $t = 0$  and is widely used in systems where impulses and their derivatives are involved, such as in control systems, signal processing, or electromagnetics.

In all simulations,  $\delta(t)$  and  $\delta'(t)$  are approximated using a Gaussian function, with  $\sigma = 0.01$ . For better understanding, both approximations are illustrated in Figures 3 and 4. Since the Gaussian approximation does not depend on a limiting process as  $h \rightarrow \infty$ , it maintains a fixed, finite-width representation of the Dirac delta for computational purposes. This approach ensures numerical stability and feasibility in simulations. This are the commonly used approximations when working with continuous systems where the Dirac delta and its derivative are needed numerically.

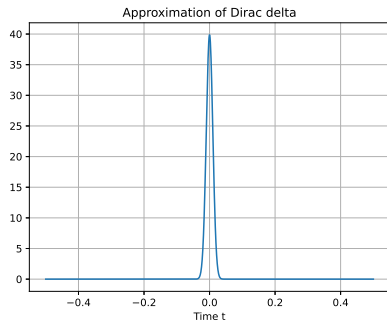


Figure 3: Dirac delta with  $\sigma = 0.01$

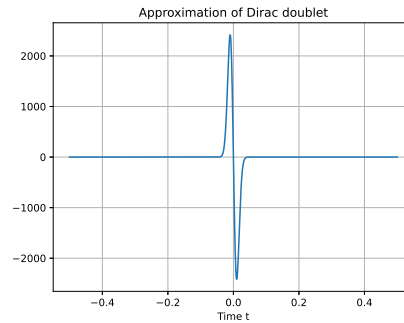


Figure 4: Dirac doublet with  $\sigma = 0.01$

To optimize the parameters of the PID controller ( $K_{p,h}, K_{i,h}, K_{d,h}$ ) using PSO method, we define the cost function as a combination of two well-known criteria, the ITAE (Integral of Time-weighted Absolute Error) and the ISO (Integral of Squared Output). The cost function  $J(K_{p,h}, K_{i,h}, K_{d,h})$  can be

expressed as a weighted combination of these two criteria. Below is a proposed formulation for this function. ITAE is defined as

$$\text{ITAE}(K_{p,h}, K_{i,h}, K_{d,h}) = \int_0^{\infty} t|e_h(t)| dt,$$

where  $e_h(t) = r(t) - y_h(t)$  is the error between the reference signal  $r(t)$  and the system output  $y_h(t)$ . The ITAE penalizes the error based on both its magnitude and the duration of the error, favoring solutions that reduce the error faster.

The ISO criterion is used to penalize overshoot in the system's response, aiming to reduce or limit the peak amplitude beyond the desired reference value during transient behavior. The integral of squared overshoot is defined as

$$\text{ISO}(K_{p,h}, K_{i,h}, K_{d,h}) = \int_0^{\infty} (\max(0, y_h(t) - r(t)))^2 dt,$$

The term  $\max(0, y_h(t) - r(t))$  captures the positive deviations or overshoot, and the square ensures that the penalty grows quadratically with the magnitude of the overshoot.

The combined cost function can be a weighted sum of ITAE and ISO, where the weights  $\lambda_{\text{ITAE}}$  and  $\lambda_{\text{ISO}}$  control the relative importance of each criterion in the optimization process. The optimization function then becomes

$$J(K_{p,h}, K_{i,h}, K_{d,h}) = \lambda_{\text{ITAE}} \cdot \text{ITAE}(K_{p,h}, K_{i,h}, K_{d,h}) + \lambda_{\text{ISO}} \cdot \text{ISO}(K_{p,h}, K_{i,h}, K_{d,h}),$$

When optimizing PID parameters, it is often impractical or unnecessary to compute these integrals over the entire infinite time domain, especially for simulations. Instead, you can define the time interval based on the duration of interest, such as the settling time or the time when significant behavior occurs in the system. This makes the optimization problem more tractable, as the integrals are computed over a finite period where the system's behavior is most relevant. Thus, the cost function in our optimization problem would be  $J(K_{p,h}, K_{i,h}, K_{d,h})$  where both ITAE and ISO are computed over the interval  $[0, T]$ ,

$$J(K_{p,h}, K_{i,h}, K_{d,h}) = \int_0^T [t|r(t) - y_h(t)| + \alpha (\max(0, y_h(t) - r(t)))^2] dt,$$

where  $\alpha > 0$  is a weighting factor that balances the reduction of overshoot with the minimization of error and  $r(t) = \eta(t)$ , the unit step function ( $\eta(t) = 1$  for  $t \geq 0$  and  $\eta(t) = 0$  for  $t < 0$ ).

This finite time approach is commonly used in numerical simulations and optimization algorithms, like PSO, to determine the best PID controller parameters.

### 8.1. Example 1: PID control for a linear first-order system

Let us consider a first-order system with dynamics defined by

$$\frac{dy(t)}{dt} + ay(t) = bu(t),$$

where the scalars  $y(t)$  is the output,  $u(t)$  is the input (control signal),  $a > 0$  is the system time constant (decay rate),  $b > 0$  is the system gain. We want to design a PID controller to ensure the system tracks a desired reference  $r(t) = \eta(t)$ . The transfer function of the system in the Laplace domain is (for  $a = 2$  and  $b = 1$ , for example)

$$G(s) = \frac{Y(s)}{U(s)} = \frac{b}{s + a} = \frac{1}{s + 2}.$$

This is a stable, first-order system with a time constant of  $\frac{1}{a} = 0.5$  seconds. A PID controller in the Laplace domain has the transfer function  $C(s) = K_p + \frac{K_i}{s} + K_d s$  and let the closed-loop transfer function is  $T(s) = \frac{C(s)G(s)}{1 + C(s)G(s)}$ . We design the PID parameters ( $K_p$ ,  $K_i$ ,  $K_d$ ) based on desired closed-loop performance specifications. For a first-order system like this, straightforward approach is closed-loop tuning [1],  $K_p = \frac{1.2}{bT} = \frac{1.2}{1 \cdot 0.5} = 2.4$ ,  $K_i = \frac{2}{T} = \frac{2}{0.5} = 4.0$ ,  $K_d = \frac{0.5T}{b} = \frac{0.5 \cdot 0.5}{1} = 0.25$ . The controller transfer function is  $C(s) = 2.4 + \frac{4.0}{s} + 0.25s$ .

The control flow comparison for the PID controller parameters, determined using the closed-loop tuning method and the PSO algorithm is presented in Figures 5 and 6.

**Remark 2.** The system under consideration is linear; hence,  $\text{Lin}_h(y) = f(y)$ , for  $y \in \mathbb{R}$  and any chosen partition parameter  $h$ .

**Remark 3.** When solving the ODE

$$1.25y'' + 4.4y' + 4y = 0.25\delta'(t) + 2.4\delta(t) + 4\eta(t),$$

the unit step response generally described in (9) with  $y(0^-) = 0$  and  $y'(0^-) = 0$  using the Laplace transform, there are a few issues that can lead to discrepancies between the solution and the initial conditions or the ODE itself.

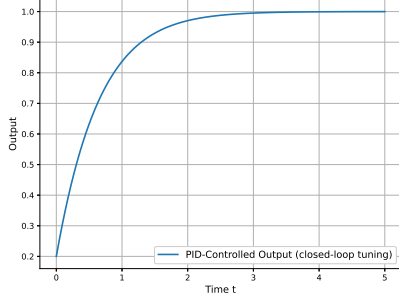


Figure 5:  $C(s) = 2.4 + \frac{4.0}{s} + 0.25s$ . PID-Controlled Output (closed-loop tuning), ITAE+ISO criterion ( $\alpha = 2000$ ): error 3.3411

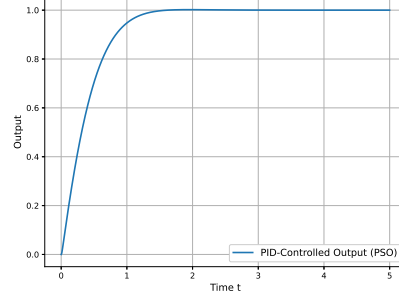


Figure 6:  $C(s) = 3.72 + \frac{10.0}{s} + 0.0s$ . PID-Controlled Output (PSO), ITAE+ISO criterion ( $\alpha = 2000$ ): error 0.1327, 5 iterations, swarm size=30,  $(K_{p,h}, K_{i,h}, K_{d,h}) \in [0, 10]^3$ .

These issues are typically related to how the Dirac delta and its derivative are handled in the Laplace transform process. When  $\delta(t)$  and  $\delta'(t)$  appears on the right-hand side, it modifies the initial conditions of the ODE. Specifically, the term  $0.25\delta'(t)$  introduces a discontinuity in  $y'(t)$ , so the initial derivative  $y'(0^+)$  is no longer 0, even if  $y'(0^-) = 0$ . Similarly,  $\delta(t)$  modifies  $y(0^+)$ , making it nonzero. Thus, the initial conditions after  $t = 0$  (i.e.,  $y(0^+)$  and  $y'(0^+)$ ) must be carefully derived by integrating the ODE across  $t = 0$ . The Dirac delta and its derivative have the following properties:

$$\int_{0^-}^{0^+} \delta(t) dt = 1.$$

This is because the Dirac delta integrates to 1 over any interval containing  $t = 0$ . For the derivative of the Dirac delta

$$\int_{0^-}^{0^+} \delta'(t) dt = \delta(t) \Big|_{0^-}^{0^+} = 0$$

because  $\delta(t)$  is defined to be zero outside  $t = 0$ .

Now analyze left-hand side across  $t = 0$ . The derivative  $y''$  contributes discontinuities in  $y'(t)$ ,

$$\int_{0^-}^{0^+} y''(t) dt = y'(0^+) - y'(0^-),$$

analogously, the derivative  $y'(t)$  contributes discontinuities in  $y(t)$ ,

$$\int_{0^-}^{0^+} y'(t) dt = y(0^+) - y(0^-),$$

and  $\int y(t)$  is continuous, so

$$\int_{0^-}^{0^+} y(t) dt = 0.$$

Substituting and equating both sides, we obtain

$$1.25y'(0^+) + 4.4y(0^+) = 2.4. \quad (11)$$

From the unit step response of this system using the transfer function,

$$Y(s) = \frac{T(s)}{s} = \frac{K_d s^2 + K_p s + K_i}{(1 + K_d)s^3 + (2 + K_p)s^2 + K_i s} = \frac{0.25s^2 + 2.4s + 4.0}{1.25s^3 + 4.4s^2 + 4.0s}.$$

using the initial-value theorem (4), we evaluate the post-initial value  $y(0^+)$  as  $\lim_{s \rightarrow \infty} sY(s) = y(0^+) = 0.2$ . Thus,  $y'(0^+) = 1.216$ , from (11).

Taking the inverse Laplace transform of  $Y(s)$ , the time-domain representation of the unit step response is

$$y(t) = \mathcal{L}^{-1}\{Y(s)\} = 1 - \frac{4}{5}e^{-\frac{44t}{25}} \cos\left(\frac{8t}{25}\right) - \frac{3}{5}e^{-\frac{44t}{25}} \sin\left(\frac{8t}{25}\right),$$

but as we can easily verify, this function does not satisfy the differential equation, nor the initial conditions. The true solution that satisfies both the equation and the initial conditions is  $y_{\text{true}}(t) = y(t)\eta(t)$ . This fact can be verified using the following rules for smooth function  $g(t) = y(t)$

$$\begin{aligned} \eta'(t) &= \delta(t), & \eta''(t) &= \delta'(t), \\ \delta(t)g(t) &= \delta(t)g(0), \\ \delta'(t)g(t) &= \delta'(t)g(0) - \delta(t)g'(0). \end{aligned}$$

**Remark 4.** This method represents a generally applicable approach for analyzing  $n$ -th order nonlinear systems by utilizing the model (8) and the principles of infinitesimal calculus as outlined in Remark 3.

For the case  $n = 1$ , the solution yields the following expressions:

For the initial jump at  $t = 0^+$ :

$$y(0^+) = \frac{K_d}{1 + K_d},$$

the system's initial response depends on how the derivative term influences the system's dynamics at  $t = 0^+$ .

For the rise slope of the response at  $t = 0^+$ :

$$y'(0^+) = \frac{K_p - aK_d}{(1 + K_d)^2}.$$

This is the instantaneous rate of change in the system's output just after the input is applied.

Thus, the exact solution of equation (9), applied to Example 1 with initial conditions  $y(0^-) = 0$ ,  $y'(0^-) = 0$ , and PID settings as specified in Figure 6 ( $K_p = 3.72$ ,  $K_i = 10$ ,  $K_d = 0$ ), yields a zero initial jump at  $t = 0^+$  due to the absence of a derivative component ( $K_d = 0$ ). Furthermore, the initial slope of the response is  $y'(0^+) = 3.72$ , corresponding to a rise angle of  $\phi = \arctan(y'(0^+)) \approx 75^\circ$ .

These results provide insight into the system's behavior during the transient response, specifically capturing the immediate effects of the initial conditions and the dynamic properties of the control parameters.

### 8.2. Example 2: PID control for a nonlinear first-order system

Consider the nonlinear first-order system given by

$$y'(t) + f(y(t)) = u(t), \quad t \geq 0,$$

where the function  $f(y)$  is defined as

$$f(y) = 0.5y + \ln(1 + y^2).$$

The function  $f(y)$  belongs to the class  $C^2(\mathbb{R} \rightarrow \mathbb{R})$ , ensuring it is twice continuously differentiable on  $\mathbb{R}$ . Furthermore,  $f(y)$  exhibits the following properties

$f(y) \rightarrow \infty$  as  $|y| \rightarrow \infty$ , indicating unbounded growth.

Both the first derivative  $f'(y)$  and the second derivative  $f''(y)$  are globally bounded on  $\mathbb{R}$ . Specifically,

$$|f'(y)| \leq 1.5 \quad \text{and} \quad |f''(y)| \leq 2, \quad \forall y \in \mathbb{R}.$$

Let the interval of linearization  $D \subset \mathbb{R}$  be chosen as  $D = [-3, 3]$ . If, during the simulation, we observe that the output  $y_h$  of the closed-loop control system approaches the boundary of the domain  $D$ , the interval  $D$  will be expanded as needed.

Assume  $h = 6$ , meaning the interval  $D$  is divided into 6 subintervals. The piecewise linear approximation of the nonlinear function  $f(y) = 0.5y + \ln(1 + y^2)$  is given as follows, see also Figure 7,

1.  $\text{Lin}_{6,1}(y) = -0.19(y + 3) + 0.80, C_{6,1} = [-3, -2]$
2.  $\text{Lin}_{6,2}(y) = -0.42(y + 2) + 0.61, C_{6,2} = [-2, -1]$
3.  $\text{Lin}_{6,3}(y) = -0.19(y + 1) + 0.19, C_{6,3} = [-1, 0]$
4.  $\text{Lin}_{6,4}(y) = 1.19(y - 0) + 0.00, C_{6,4} = [0, 1]$
5.  $\text{Lin}_{6,5}(y) = 1.42(y - 1) + 1.19, C_{6,5} = [1, 2]$
6.  $\text{Lin}_{6,6}(y) = 1.19(y - 2) + 2.61, C_{6,6} = [2, 3]$ .

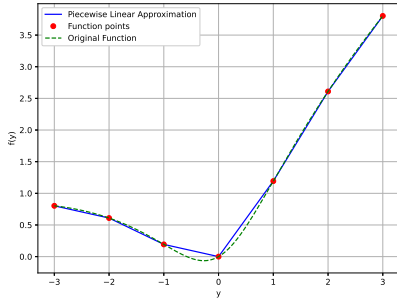


Figure 7:  $f(y) = 0.5y + \ln(1 + y^2)$  and its piecewise linear approximation  $\text{Lin}_{h=6}(y)$ .

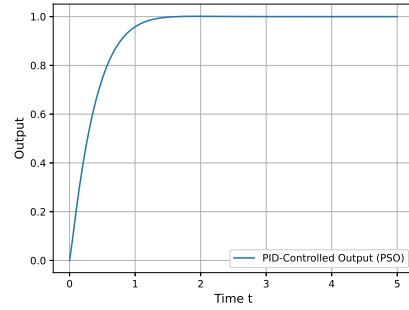


Figure 8:  $C(s) = 4.65 + \frac{10}{s} + 0.0s$ . PID-Controlled Output (PSO), ITAE+ISO criterion ( $\alpha = 2000$ ): error 0.1121, 10 iterations, swarm size=30,  $(K_{p,h}, K_{i,h}, K_{d,h}) \in [0, 10]^3$ .

The overall piecewise linear approximation is denoted as

$$\text{Lin}_h(y) \triangleq \{\text{Lin}_{h=6,i}(y) \mid i = 1, 2, \dots, 6\}.$$



and the progression of the piecewise linearized control process is depicted in Figure 8.

Expanding  $D$  dynamically ensures that the simulation remains valid for a wide range of system responses. However, it also increases computational complexity. Choosing an appropriate initial domain  $D$  is important to minimize unnecessary expansions. Dividing  $D$  into 6 equal subintervals simplifies the linearization process while maintaining a good approximation of the original nonlinear function  $f(y)$ . Increasing  $h$  (more subdivisions) would improve the accuracy of the approximation but would also add computational overhead. Since  $f(y)$  is being replaced by its piecewise linear approximation  $\text{Lin}_h(y)$ , the system retains a globally Lipschitz structure.

As we might have noticed that for the first-order systems without time delay, the derivative component is not required to achieve the setpoint. A PI controller is sufficient to handle both transient and steady-state performance. On the contrary, as we have observed, its presence causes an initial jump for first-order systems. The derivative component becomes relevant for higher-order systems where it helps dampen oscillations or overshoot caused by complex dynamics.

## 9. Conclusions

In conclusion, the use of piecewise linear approximation for nonlinear systems provides an effective method for simplifying the analysis and control of the system. By approximating the nonlinear function with linear pieces over simplices, we maintain the essential properties necessary for stable control, such as Lipschitz continuity. This ensures that the system's behavior remains predictable and bounded, which is crucial for stability in feedback control systems.

Moreover, the approximation allows the use of well-established control techniques, such as PID control, while ensuring that the system behaves in a manner that is consistent with its nonlinear nature, especially as the approximation becomes more refined with higher  $h$ . Increasing  $h$  leads to a more accurate piecewise linear approximation of the nonlinear function, which in turn results in a better representation of the nonlinear system. This improved approximation enhances the performance of control systems, such as PID controllers, by minimizing the error between the linearized model and the original nonlinear system. However, this comes at the cost of higher

computational complexity, so a balance must be struck between accuracy and efficiency based on the specific application.

Overall, the approach makes nonlinear systems more tractable while preserving their core dynamic characteristics, enabling more effective control and analysis in practical applications.

### **Declaration of Generative AI and AI-assisted technologies in the writing process**

During the preparation of this work the author(s) used ChatGPT in order to improve readability and language of the manuscript. After using this tool, the author(s) reviewed and edited the content as needed and take(s) full responsibility for the content of the publication.

### **References**

- [1] K. J. Astrom and T. Haggund. *PID Controllers: Theory, Design, and Tuning*. ISA - The Instrumentation, Systems and Automation Society, Research Triangle Park, North Carolina, 1995.
- [2] K. J. Astrom and T. Haggund. *Advanced PID Control*. ISA-The Instrumentation, Systems, and Automation Society, Research Triangle Park, North Carolina, 2006.
- [3] S. Banach. Sur les operations dans les ensembles abstraits et leur application aux equations integrales. *Mathematische Annalen*, 98(1):1–88, 1922.
- [4] R. L. Burden and J. D. Faires. *Numerical Analysis*. Brooks/Cole, Cengage Learning, Boston, MA, 9th edition, 2010. Youngstown State University.
- [5] C. A. Coello Coello and M. S. Lechuga. Mopso: A proposal for multiple objective particle swarm optimization. In *Proceedings of the IEEE Congress on Evolutionary Computation*, pages 1051–1056, 2002.
- [6] K. Deb and H. Jain. An evolutionary many-objective optimization algorithm using reference-point-based nondominated sorting approach, part i: Solving problems with box constraints. *IEEE Transactions on Evolutionary Computation*, 18(4):577–601, 2013.

- [7] R. C. Eberhart and J. Kennedy. Particle swarm optimization. In *Proceedings of IEEE International Conference on Neural Networks*, pages 1942–1948, 1995.
- [8] T. H. Gronwall. Note on the derivatives with respect to a parameter of the solutions of a differential equation. *Annals of Mathematics*, 20(1):292–296, 1919.
- [9] J. Kennedy and R. C. Eberhart. A discrete binary version of the particle swarm algorithm. In *Proceedings of the IEEE International Conference on Systems, Man, and Cybernetics*, pages 4104–4108, 1997.
- [10] K. H. Lundberg, H. R. Miller, and D. L. Trumper. Initial conditions, generalized functions, and the Laplace transform: Troubles at the origin. *IEEE Control Systems Magazine*, 27(1):22–35, 2007.
- [11] N. S. Nise. *Control Systems Engineering*. Wiley, Hoboken, NJ, 6th edition, 2011.
- [12] K. Ogata. *Modern Control Engineering*. Pearson, Upper Saddle River, NJ, 5th edition, 2010.
- [13] A. Papoulis. *The Fourier Integral and Its Applications*. McGraw-Hill, first edition, 1962.
- [14] R. Poli, J. Kennedy, and T. Blackwell. Particle swarm optimization. *Swarm Intelligence*, 1(1):33–57, 2007.
- [15] M. Schetzen. *The Volterra and Wiener Theories of Nonlinear Systems*. John Wiley & Sons, New York, 1980.
- [16] Y. Shi and R. C. Eberhart. A modified particle swarm optimizer. In *Proceedings of the IEEE International Conference on Evolutionary Computation*, pages 69–73, 1998.
- [17] D. Wang, D. Tan, and L. Liu. Particle swarm optimization algorithm: an overview. *Soft Computing - A Fusion of Foundations, Methodologies and Applications*, 22(2):387–408, 2018.